8 (a). Microbial mats built by iron bacteria: a modern example from southern Indiana

Juergen Schieber and Mihaela Glamoclija

Iron biominerals comprise approximately 40% of all minerals formed by organisms (Lowenstam, 1986; Bazylinski and Frankel, 2003 p. 6), and play an important role in biogeochemical redox reactions of marine and fresh water environments. Biogenic iron oxides have been the focus of a number of studies in recent years (e.g., Straub et al., 2001; Emerson and Weiss, 2004; Kappler and Newman, 2004; Fortin and Langley, 2005), and their most common forms include oxides (magnetite, hematite), oxyhydroxides (e.g., goethite, akagenite, lepidocrocite) and poorly ordered phases (Cornell and Schwertmann, 2003). Amorphous iron, ferrihydrite and lepidocrocite have been identified in association with bacterial cell walls and extracellular polymers in fresh water environments (e.g., Tipping et al., 1989; Fortin et al., 1993), wetlands (e.g., Emerson et al., 1999), iron-rich seepage areas (James and Ferris, 2004), as well as in deep aquifers (Hallberg and Ferris, 2004). Studies of vent systems around the world show that amorphous iron-oxides and ferrihydrite are commonly associated with bacteria (see review article by Little et al., 2004).

Biotic reactions that form iron-oxides include microbial oxidation of Fe(II) to Fe(III), and depend on pH and O_2 concentrations. In pH neutral environments *Gallionella* spp. and *Leptothrix* spp. are common microaerophilic bacterial species involved in biogenic iron oxidation (Emerson and Weiss, 2004). Whether and how these bacteria derive energy from the oxidation of Fe(II) while in competition with rapid abiotic oxidation of Fe(II) at neutral pH is still a matter of debate (Sobolev and Roden, 2004), but the intimate association of iron precipitation and microbial extracellular polymer material (EPS) suggests that they most likely do derive some benefit. Chemolithotrophy of Fe-oxidizing bacteria in pH neutral environments provides at least a partial rationale (Hallbeck and Pedersen, 1991). For example, iron oxidation by *Gallionella* shows close spatial correlation with stalk production because the organism continuously produces fresh stalk material in order to nucleate iron oxides and thus to gain energy for survival (Anderson and Pedersen, 2003). *Leptothrix* has the ability of passive sorption of iron and iron oxides onto the sheath (Emerson and Weiss, 2004), yet it remains difficult to clearly differentiate between true biogenic Fe-oxides and those formed as a result of abiotic reactions.

A better appreciation of iron oxidizing bacteria may be vital for understanding the processes that formed Archaean and Proterozoic banded iron formations (BIF), deposits that are critical for reconstructing the early evolution of Earth's atmosphere. While there are multiple hypotheses to explain these deposits (e.g., Holland, 1973; Morris and Horwitz, 1983; Isley, 1995; Rasmussen and Buick, 1999), the potential role of iron oxidizing bacteria has yet to be evaluated seriously in these scenarios.

The current understanding is that oxygenic photoautotrophs forced the oxidation of ferrous iron in ancient depositional basins via the production of molecular oxygen

In: *Atlas of microbial mat features preserved within the clastic rock record*, Schieber, J., Bose, P.K., Eriksson, P.G., Banerjee, S., Sarkar, S., Altermann, W., and Catuneau, O., (Eds.), Elsevier, p. 233-244. (2007)

(Pierson et al., 1999; Kamber et al., 2004). Because the biochemical pathways necessary to deal with molecular oxygen had not yet evolved, oxygenic photoautotrophs of the time would have depended on the ready availability of ferrous iron to "neutralize" the toxic oxygen they produced (Cloud, 1973). Alternatively, ferrous iron might have been oxidized via early anaerobic photosynthesis (Pierson et al., 1999). Iron-oxidizing bacteria gain energy from the oxidation of ferrous iron and offer an alternative or additional pathway (in addition to photosynthetic production of O_2) of iron oxidation and deposition. For example, bacterial stalks of *Gallionella* spp. and *Gallionella*-like organisms almost completely compose iron-rich layers near the exhalative zone of a shallow hydrothermal vent near the island of Santorini and near the hydrothermal outflows in Iceland (Holm, 1987). Iron oxidation by microaerophilic species (*Gallionella* and *Chromatium*) that can occupy ecological niches with limited O_2 availability has been proposed as a mechanism for widespread deposition of ferric iron in BIF's (Holm, 1989; Konhauser et al., 2002). Iron-reducing bacteria were suggested as a third group of organisms involved in the formation of BIF's. The hypothesis derives from the observation that within BIF's, iron-poor layers with carbonates contain isotopically light carbon. The source of that light carbon may have been remains of phototrophic organisms that accumulated on the surface of oxidized iron layers (Baur et al., 1985; Nealson and Myers, 1990).

For all these reasons it is essential to better understand the textural and isotopic biosignatures of iron oxidizing bacteria, and we are therefore currently studying a modern system where *Gallionella* and *Leptothrix* produce copious quantities of iron oxides under constantly fluctuating environmental conditions. Studying the processes and dynamics of this system may eventually provide critical new insights into mechanisms that may have produced the banded iron formations of the past.

Our study site, a groundwater-fed small creek near Bloomington/Indiana, USA, is characterized by prominent reddish-brownish deposits of iron hydroxides. The water seeps into the creek from a sandstone horizon within the Mississippian Borden Formation, a succession of marine marls, carbonates, and sandstones. These sediments contain variable amounts of diagenetic pyrite that is oxidized as surface waters percolate through the sediments. In the process, iron goes into solution as ferrous iron (the Fe^{2+} ion). Discharge of these iron-rich waters is intimately linked to an occurrence of masses of iron bacteria. Under the given environmental conditions, iron bacteria oxidize Fe(II) and gain energy according to the following reaction:

$$Fe^{2+} + 0.25O_2(aq) + 2.5H_2O \rightarrow Fe(OH)_3(s) + 2H^+$$
$$\Delta G^{\circ\prime} = -111.3\ kJ/e^-$$

where $\Delta G^{\circ\prime}$ is the overall amount of energy available for cellular metabolism at neutral pH.

This reaction occurs at redox interfaces where diffusion-limited O_2 transport leads to low dissolved O_2 partial pressure (microaerobic conditions) within the zone of Fe(II)-O_2 overlap (Roden et al., 2004). With continued reaction the iron bacteria at our study site

In: *Atlas of microbial mat features preserved within the clastic rock record*, Schieber, J., Bose, P.K., Eriksson, P.G., Banerjee, S., Sarkar, S., Altermann, W., and Catuneau, O., (Eds.), Elsevier, p. 233-244. (2007)

form loaf-shaped and bulbous buildups, as well as flat to undulose mats that cover the creek bed (Fig. 8(a)-1A). The sheath-forming bacterium *Leptothrix* dominates, but spiral stalks of *Gallionella* are common and can be abundant during certain growth stages (Fig. 8(a)-4). Microbial growth forms are fragile and of the consistency of custard. During rainstorms, when surface runoff dominates creek flow, they can be partially or completely eroded depending on the intensity of rainfall (Fig. 8(a)-1B).

Mat erosion produces partially eroded mat remnants (Fig. 8(a)-2A), upturned and flipped-over edges of mats (Fig. 8(a)-1B; Fig. 8(a)-2C), mat roll-ups (Fig. 8(a)-2B) as known from other microbial mat occurrences (e.g., Schieber, 1999; Simonson and Carney, 1999), large quantities of irregularly shaped and sized mat fragments (Fig. 8(a)-2A), and surface wrinkles due to current drag on the mat surface (Figs. 8(a)-2C and -2D). The latter effect actually produces a morphology that resembles the "elephant skin" texture described from microbial mats on sandy substrates (e.g., Gehling, 1999; see also Chapter 6(a)). Sediment transport during high-flow interludes can deposit sand and clay on mat surfaces that are strong enough to resist erosion (Figs. 8(a)-2C, -2D, and -2E). Sediment accumulation on these mats can produce macroscopically recognizable internal laminae (Fig. 8(a)-5E) and opens up the potential for the generation of stromatolite-like structures that have long term preservation potential (Fig. 8(a)-5).

Re-growth of iron microbial mats is vigorous and full mat coverage after storm washout is typically achieved within a week (Fig. 8(a)-3A). A large portion of the mat structure consists of iron hydroxide encrusted sheaths of *Leptothrix,* shed constantly by this organism as it multiplies. The sheaths themselves are composed of polysaccharide based materials, and as growth continues there is a rapid buildup of organic matter that provides food for other microorganisms. Thus, mats that form early in a post-washout growth cycle may show signs of decay and disintegration within a few days of their formation (Figs. 8(a)-3A and -3C). It is at this point in mat development that a different growth form, light coloured streamlined clumps, appears superimposed on the earlier mat (Figs. 8(a)-3A, -3B, and -3C). The observation that the best growth of these secondary growth forms occurs where flow is swiftest (Fig. 8(a)-3B), suggests a response of the microbial community to the flux density of essential water borne nutrients such as dissolved organic compounds and dissolved iron. Better mixing with surface oxygen in the more turbulent fast flowing sections of the creek is likely a contributing factor. Somewhat deeper portions of the creek with a water depth of a few centimetres to 20 cm are the preferred site of growth for thicker mat developments (Fig. 8(a)-1). In steeper portions of the creek the flow is very fast and consequently the water cover is only a few millimetres to perhaps a centimetre in thickness. Under those conditions the mat cover is only a few millimetres thick at best (Fig. 8(a)-3D) and may peel off as thin crumbled sheets (Fig. 8(a)-3E) when eroded.

As summarized above, the iron microbial community in this creek shows morphologic response to changes in flow velocity, recycling of organic matter in the environment, flow depth influences and other factors. Whereas the above-described responses are clearly visible at the macroscopic level, they are most likely also reflected in the microscopic structure of these mats. The work on that aspect of the system is still in

progress, but a few observations are presented here (Fig. 8(a)-4) to illustrate the finer details of mat construction.

Mat surfaces show three basic ingredients (Fig. 8(a)-4), *Leptothrix* sheaths, twisted *Gallionella* stalks, and extracellular polymer substance (EPS). In places either one of these may be found to dominate the mat surface (Fig. 8(a)-4A, -4B, and -4F). Iron microbe layers show a considerable degree of internal organization at the microscopic level. Freeze dried samples, freeze-fractured perpendicular to macroscopic lamination, show a fine scale layering consisting of "storeys" of matted *Leptothrix* sheaths that exhibit regular spacing of some ten microns (Fig. 8(a)-4C and -4D). The "storeys" seem to be held apart by other *Leptothrix* sheaths that are oriented at steep angles to the planes defined by the "storeys". These structural elements are held together by a carbon-rich and iron hydroxide encrusted matrix, presumably EPS. This structural style actually shows an uncanny resemblance to bamboo scaffolding that one sees in many Asian cities, delicate appearing structures of surprising strength that consist of bamboo poles tied together by ropes. On breaks parallel to lamination it becomes clear that what holds the "storeys" apart is a honeycomb structure of entwined *Leptothrix* sheaths, *Gallionella* stalks, unidentified filaments, and more EPS (Fig. 8(a)-4E). The outermost microlamina, the actual growth surface of the mat at the time of collection, shows in addition to *Leptothrix* sheaths and *Gallionella* stalks a surface texture that has the appearance of thin sheets of a stretchable substance criss-crossing and covering "holes" not occupied by sheaths and stalks (Fig. 8(a)-4E). The stretched sheets consist of an organic matrix (probably EPS) that is encrusted with nanoscale balls of iron hydroxides (Fig. 8(a)-4E).

It appears thus that the observed mats consist of a framework in which stiff, mineralized *Leptothrix* sheaths are probably the dominant load-carrying elements. This framework compartmentalizes the occupied volume into numerous hollow spaces that are filled with water. The EPS matrix that holds the structural elements together also prevents, or at least severely limits, water exchange between compartments. Production of EPS requires energy and nutrients, and by following the observed building strategy the microbes conserve resources while still increasing their structural surface to support a growing population.

In order to examine how iron microbial mats as described above may appear in the rock record, selected spots on the creek bed were marked with PVC tubing (Fig. 8(a)-5A) and the area repeatedly sprinkled with fine sand (Fig. 8(a)-5B) to produce easily recognizable laminae within the growing mat. After collecting the mat sample contained in the PVC tubing, a portion of the mat was shock frozen in liquid nitrogen and freeze dried (Fig. 8(a)-5C), and another portion was infused with Spurr resin, cured, and then ground and polished (Fig. 8(a)-5D). Both preparation methods show preserved layering (Figs. 8(a)-5C and -5D). Even though the mat is constructed very lightly (Fig. 8(a)-4), it is able to support the weight of sand layers that are several mm thick (Fig. 8(a)-5D). That this type of lamination can indeed occur naturally is illustrated by Fig. 8(a)-5E. Thus, iron microbial mats can form potentially preservable stromatolites. Preservation potential is probably greatly enhanced by rapid burial with other sediments. Alternatively, if eroded mat material is for example washed into a lake basin, it could form deposits of

In: *Atlas of microbial mat features preserved within the clastic rock record*, Schieber, J., Bose, P.K., Eriksson, P.G., Banerjee, S., Sarkar, S., Altermann, W., and Catuneau, O., (Eds.), Elsevier, p. 233-244. (2007)

microbially precipitated iron that have unique textural attributes and could as well become part of the geological record.

Our observations demonstrate that under sufficiently dynamic environmental conditions, iron oxidizing bacteria can produce layered, stromatolite-like morphologies. The formation of stromatolite laminae may mimic processes that were present during the formation of BIF's. Ongoing *in situ* experiments are designed to help us understand microbial morphological and geochemical responses to different environmental conditions. Microbial mat deposits in multiple periods of Earth history were iron-mineralized to various degrees and may also contain remains of the organisms that formed them (LaBerge, 1973; Gerdes and Krumbein, 1987; Schieber, 1989, 2002; Konhauser et al., 2002). The common association of microbes and iron accumulations on Earth holds out the prospect that a similar association may exist on Mars as well. Thus, Martian hematite accumulations, such as those of Meridiani Planum (Christensen et al., 2000), are currently favoured targets in the search for ancient microbial life on that planet.

In: *Atlas of microbial mat features preserved within the clastic rock record*, Schieber, J., Bose, P.K., Eriksson, P.G., Banerjee, S., Sarkar, S., Altermann, W., and Catuneau, O., (Eds.), Elsevier, p. 233-244. (2007)

Figures and Captions: Chapter 8(a)

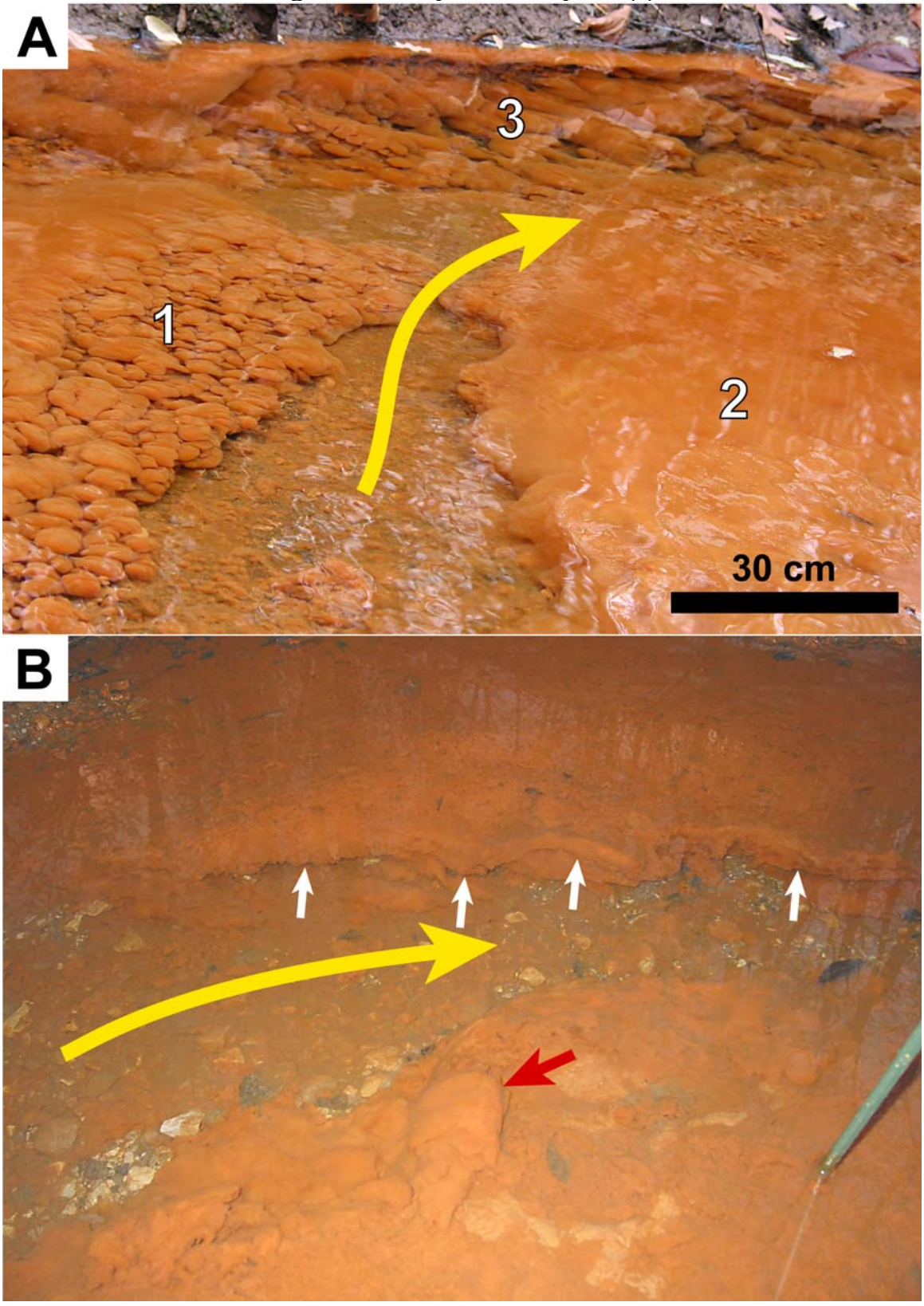

In: *Atlas of microbial mat features preserved within the clastic rock record*, Schieber, J., Bose, P.K., Eriksson, P.G., Banerjee, S., Sarkar, S., Altermann, W., and Catuneau, O., (Eds.), Elsevier, p. 233-244. (2007)

Figure 8(a)-1: Two views of creek bed with iron bacterial mat. Scale approximate, scale bar applies to both images:

(A) Shows active growth stage of mat. At left, in the area of stronger current, we see development of a field of bulbous mat buildups (marked 1). At right, in an area of weaker current, we see development of an essentially planar mat (marked 2). The creek channel is curving to the right (yellow arrow). At the far side of the image, the cut bank of the channel which suffers erosion during maximum flow, microbial buildups are inclined (marked 3) at approximately 30 degrees to the right. This inclination probably reflects the downwelling of the current that is typical for flow in stream channels (Reineck and Singh, 1980). (B) Appearance of mat after erosive event (rainstorm). The central channel where the swiftest flow is concentrated (yellow arrow) has been swept clean and is in the process of mat resurfacing. The edge of the mat has been eroded, undercut, and partly turned up (white arrows). In the foreground we see a large mat fragment that has been rolled up (red arrow) while being transported across the mat surface.

In: *Atlas of microbial mat features preserved within the clastic rock record*, Schieber, J., Bose, P.K., Eriksson, P.G., Banerjee, S., Sarkar, S., Altermann, W., and Catuneau, O., (Eds.), Elsevier, p. 233-244. (2007)

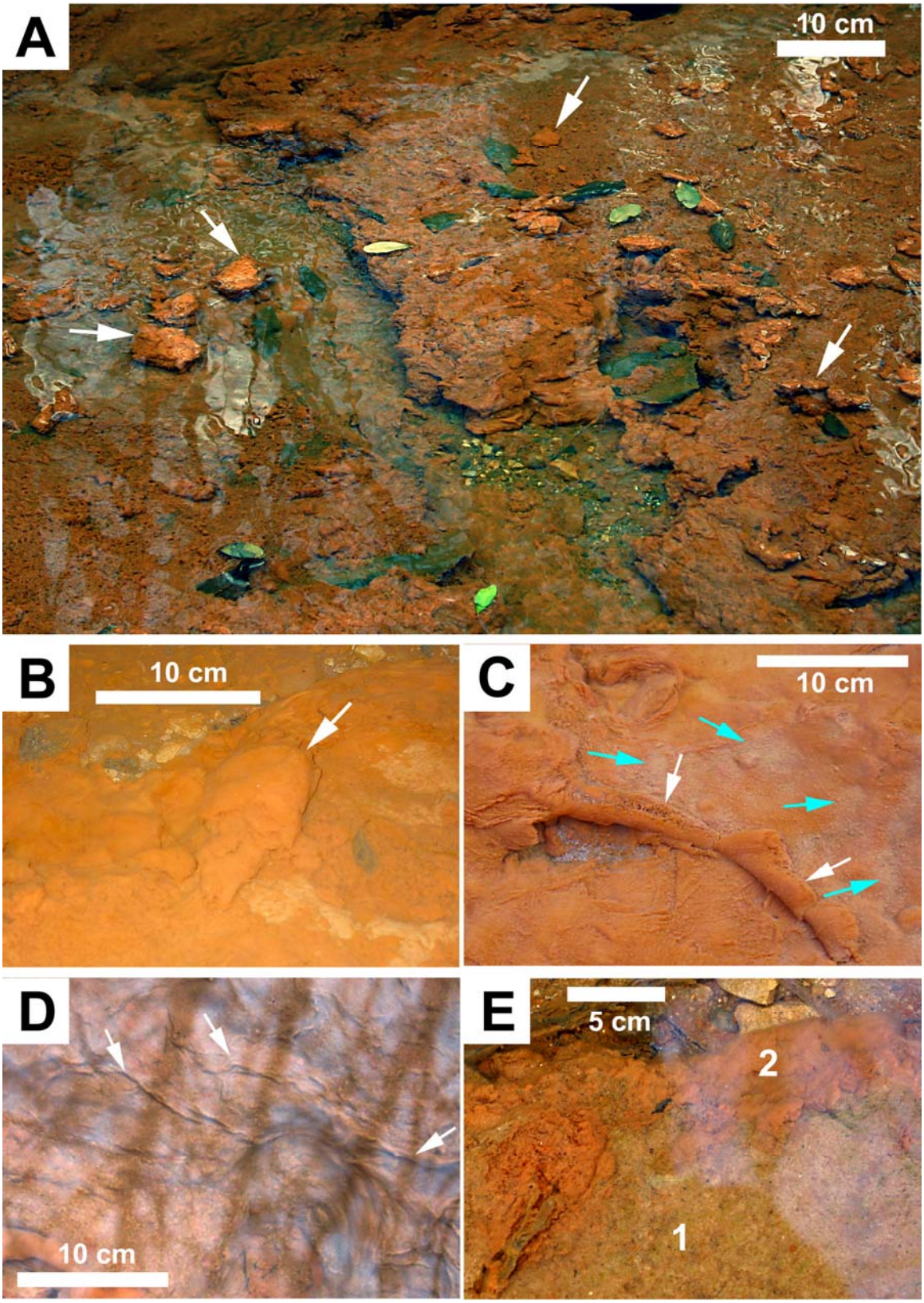

In: *Atlas of microbial mat features preserved within the clastic rock record*, Schieber, J., Bose, P.K., Eriksson, P.G., Banerjee, S., Sarkar, S., Altermann, W., and Catuneau, O., (Eds.), Elsevier, p. 233-244. (2007)

Figure 8(a)-2: Erosion related features:

(A) Partially eroded mat and ripped-up mat fragments. (B) Mat roll-up from Fig. 8(a)-1B (white arrow). (C) Multi-layered mat with the uppermost layer partially eroded and flipped over at the edge (white arrows). The mat surface has accumulated thin patches of sand (turquoise arrows) that was carried with flood waters (current from lower left to upper right). Note the wrinkled nature of the mat surface. (D) Current-wrinkled mat surface with a thin veneer of sand. The surface wrinkles on the mat (white arrows) are oriented approximately perpendicular to the current (from lower left to upper right). This may reflect creeping of the uppermost mat layer in response to bottom shear stress. (E) Eroded edge of a thick planar mat (marked 2) that is covered with a layer of sand (marked 1).

In: *Atlas of microbial mat features preserved within the clastic rock record*, Schieber, J., Bose, P.K., Eriksson, P.G., Banerjee, S., Sarkar, S., Altermann, W., and Catuneau, O., (Eds.), Elsevier, p. 233-244. (2007)

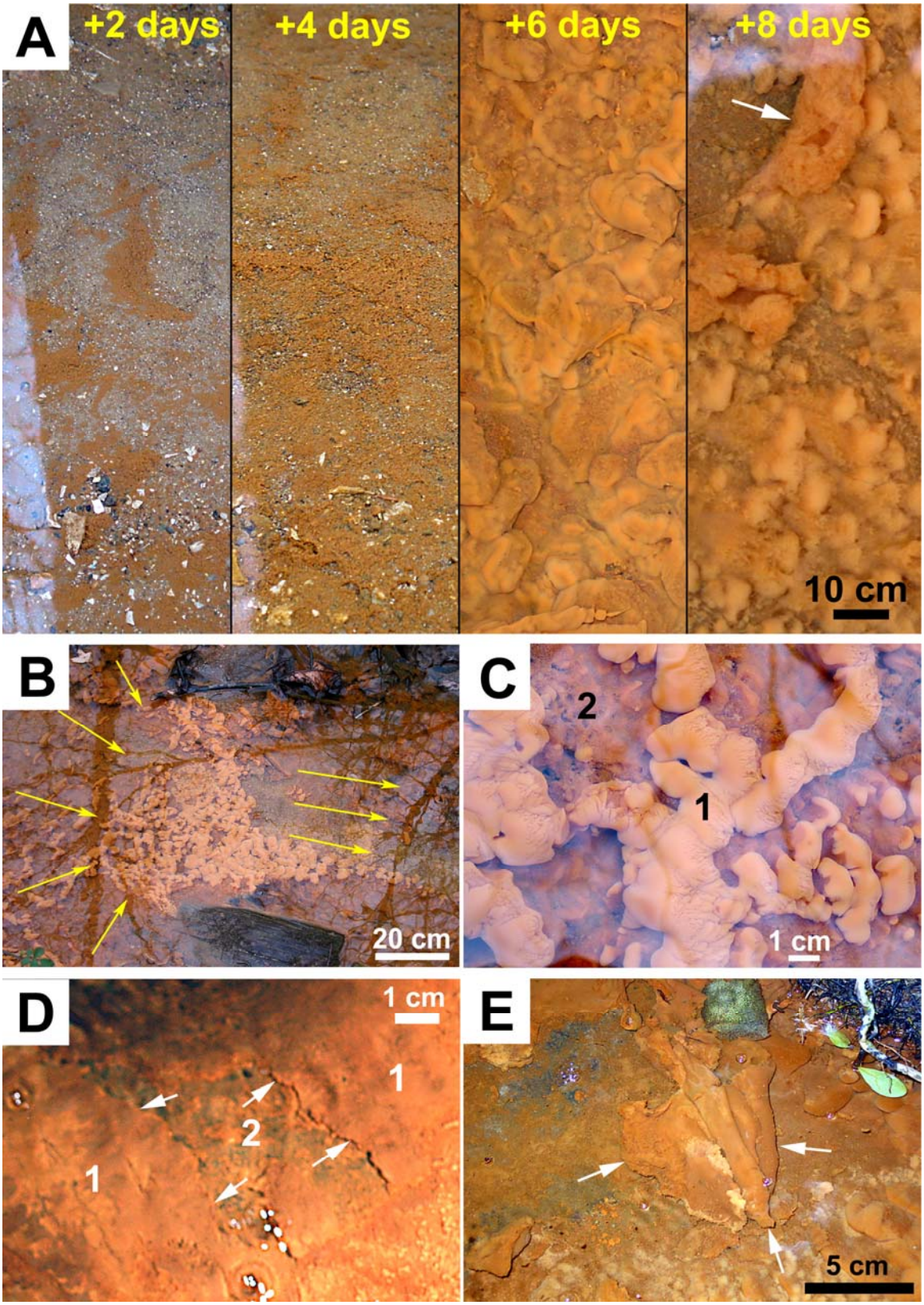

In: *Atlas of microbial mat features preserved within the clastic rock record*, Schieber, J., Bose, P.K., Eriksson, P.G., Banerjee, S., Sarkar, S., Altermann, W., and Catuneau, O., (Eds.), Elsevier, p. 233-244. (2007)

Figure 8(a)-3: Mat growth, flow velocity, and flow depth:

(A) Photos that illustrate the speed of mat recovery. The four images were taken 2 days apart; starting two days after a rainstorm had completely "washed out" the previously existing mat. Once surface runoff ends and flow is spring-fed only, small tufts of iron microbes (mostly *Leptothrix*), a few millimetres in size, start to form loose accumulations on the creek bed (+2 days). Four days after "washout" these loose accumulations start to fuse into contiguous microbially bound patches. After six days a microbial "fluff", a few millimetres thick, covers most surfaces on the creek bed. After eight days the earlier grown mat has peaked, starts to decay, and may in places peel off (arrow 1) even under weak currents. Bulbous secondary growth forms (light coloured streamlined clumps) are established on top. (B) The effect of flow constriction on mat growth. The flow in the creek is from left to right (yellow arrows), and the channel narrows to about half its width due to obstacles. Whereas upstream (far left) the initial mat (Fig. 8(a)-2A) shows a cover of scattered bulbous (light coloured streamlined clumps) growth forms, the latter grow much more densely in the area where the flow narrows (centre of image) and flow velocity is increased. (C) Detail of secondary growth forms (also referred to as light coloured streamlined clumps). Shows older decaying mat of darker reddish-brown colour (marked 2) overgrown by secondary forms (beige colour, marked 1) that are streamlined and flow oriented (flow from left to right). (D) Photo from a steeper sloping (10 to 15 degrees) portion of the creek. Under normal conditions, the water flow is only a few millimetres to 1 cm deep, and as a result the iron microbial mat only grows to a thickness of a few millimetres. Photo shows where a layer of mat (marked 1) has been scraped off the bedrock for sampling (area marked 2), and illustrates the thinness of the mat (arrows). (E) Another photo from steeper sloping (10 degrees) portion of the creek. It shows a thin mat layer (white arrows) that has just become detached from the bedrock surface and is being crumbled up by currents.

In: *Atlas of microbial mat features preserved within the clastic rock record*, Schieber, J., Bose, P.K., Eriksson, P.G., Banerjee, S., Sarkar, S., Altermann, W., and Catuneau, O., (Eds.), Elsevier, p. 233-244. (2007)

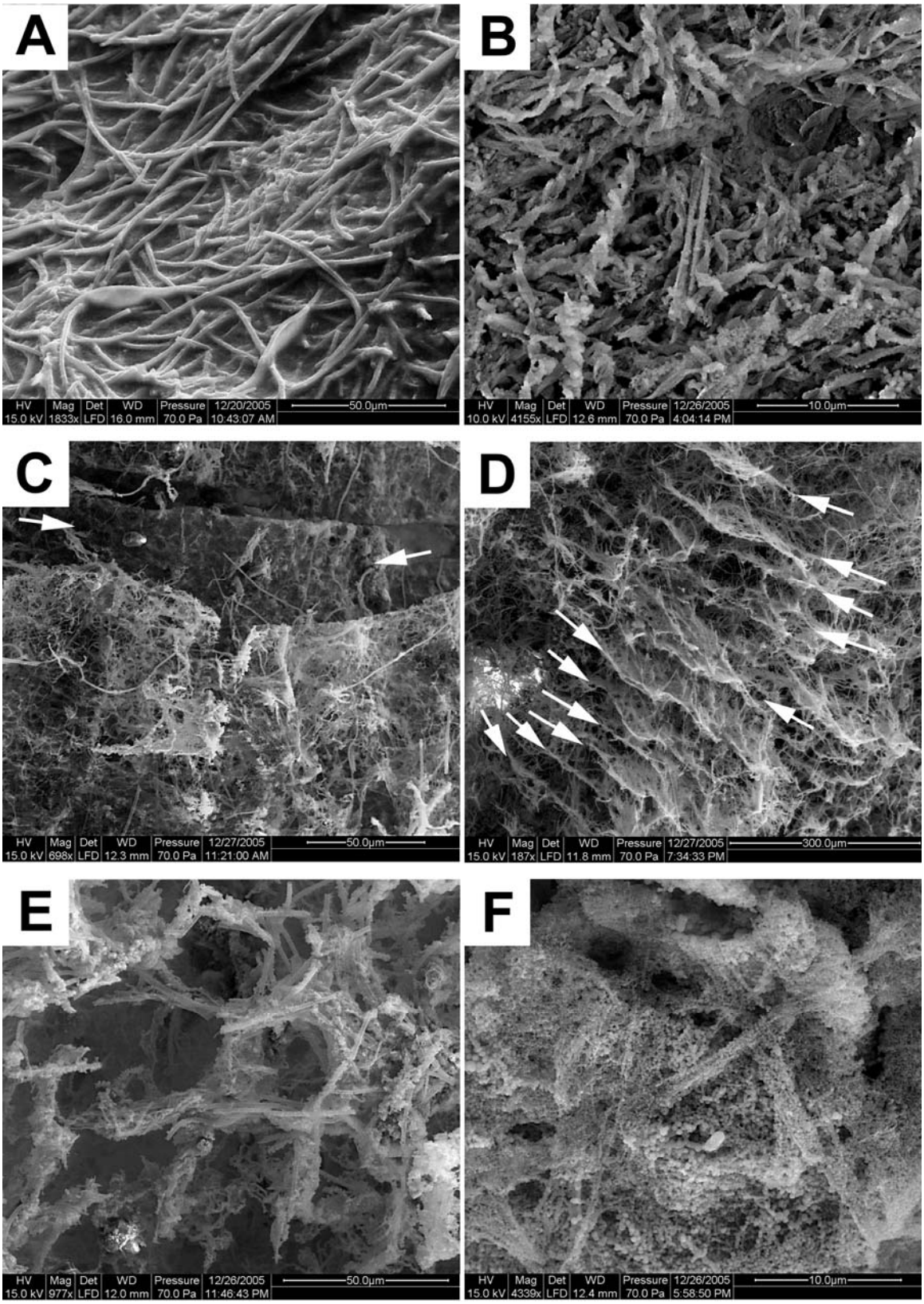

In: *Atlas of microbial mat features preserved within the clastic rock record*, Schieber, J., Bose, P.K., Eriksson, P.G., Banerjee, S., Sarkar, S., Altermann, W., and Catuneau, O., (Eds.), Elsevier, p. 233-244. (2007)

Figure 8(a)-4: Mat textures:

(A) ESEM image of *Leptothrix* dominated mat surface. Note films of EPS between filaments. (B) SEM image of another mat surface sample. This sample was shock frozen in liquid nitrogen and freeze dried. This particular sample shows an abundance of *Gallionella* stalks on the surface. (C) Lower magnification SEM top-view of a mat surface that consists of intertwined *Leptothrix* sheaths and *Gallionella* stalks in a matrix of EPS. Freeze drying reduces the EPS matrix to very thin films between filaments and stalks. The sample was fractured and shows an older mat surface beneath (arrows). Shock frozen and freeze dried sample. (D) SEM view of a fracture surface perpendicular to the mat surface. Arrows point to multiple storeys of matted *Leptothrix* sheaths that represent former mat surfaces and now give rise to an internal laminar structure. Storeys are interconnected by variably inclined (relative to storey plane) *Leptothrix* sheaths. Shock frozen and freeze dried sample. (E) SEM view of a honeycomb-like structure that consists if intertwined *Leptothrix* sheaths and *Gallionella* stalks that are held together by EPS. This is a common structural element that holds apart (separates) successive storeys. Shock frozen and freeze dried sample. (F) Detail of EPS covered surface. Strands of EPS are criss-crossing the surface and are encrusted by small round spheres that consist of precipitated iron hydroxides. These spheres are on the order of some tens to several hundred nanometres in size. Shock frozen and freeze dried sample.

In: *Atlas of microbial mat features preserved within the clastic rock record*, Schieber, J., Bose, P.K., Eriksson, P.G., Banerjee, S., Sarkar, S., Altermann, W., and Catuneau, O., (Eds.), Elsevier, p. 233-244. (2007)

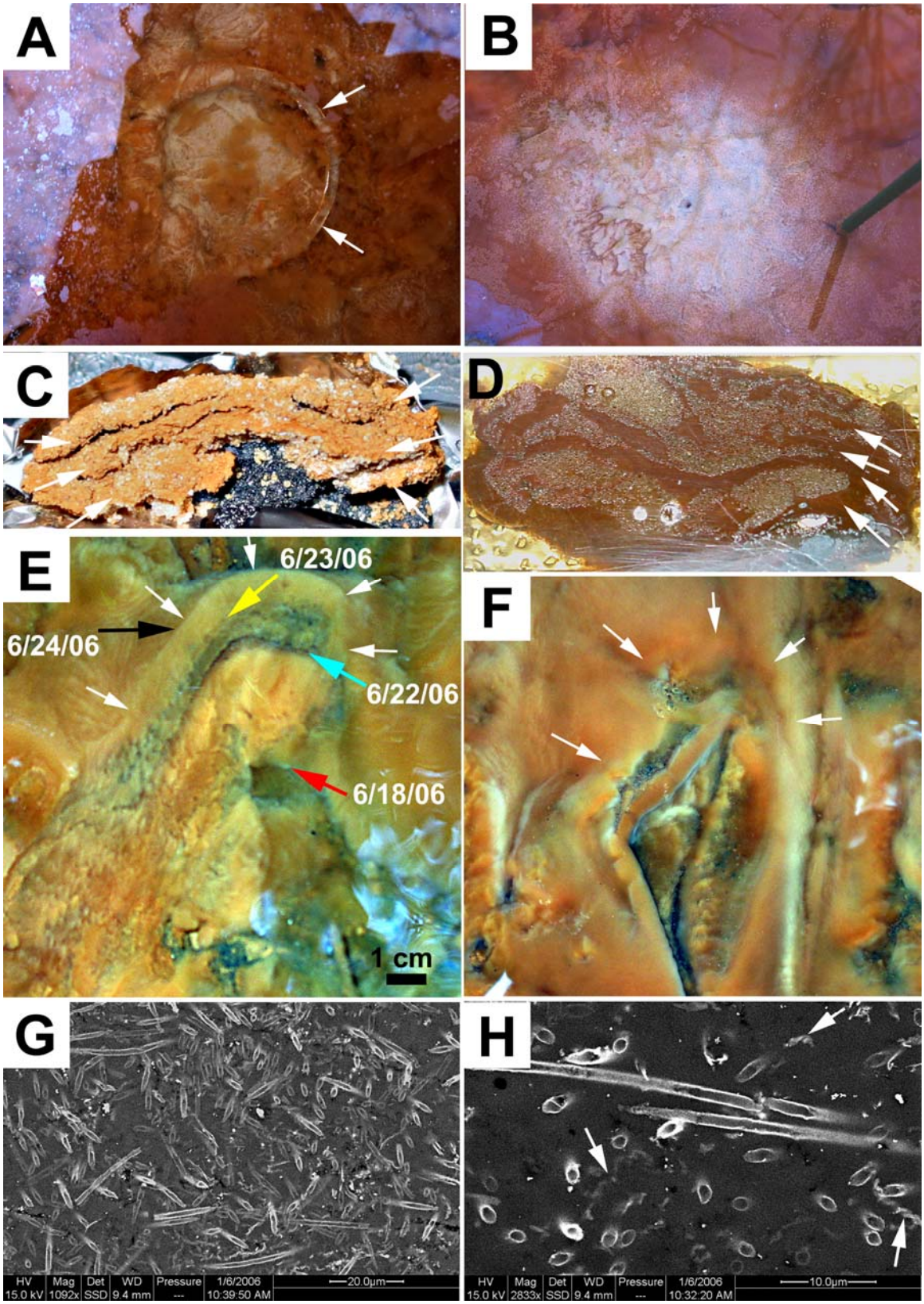

In: *Atlas of microbial mat features preserved within the clastic rock record*, Schieber, J., Bose, P.K., Eriksson, P.G., Banerjee, S., Sarkar, S., Altermann, W., and Catuneau, O., (Eds.), Elsevier, p. 233-244. (2007)

Figure 8(a)-5: Potential preservational textures:

(A) Sampling site for iron bacteria stromatolite growth test. A plastic pipe (arrows) of 10 cm diameter was buried in the creek bed and gradually raised as the mat grew in thickness. (B) Same place as in A, but with mat covering the pipe rim. In order to preserve and mark lamination, fine sand was sprinkled on the mat every few days. The mat would re-cover the sedimented area within a matter of several days. (C) Shock frozen and freeze dried sample (vertical section) of the mat in A and B. Three successive layers (arrows) are clearly visible. Scale bar is 10 mm long. (D) Another vertical section through the same mat as shown in A. This sample was soaked with Spurr resin after sectioning, cured and hardened. The resulting slab was then ground flat and polished to show internal laminae. It shows alternating reddish mat layers and sand layers (granular), as well as ball-and-pillow structures because the much denser sand was sinking down into the watery mat layers. Scale bar is 10 mm long. (E) Photo of *in situ* bulbous iron microbial mat buildup (similar to those seen in Fig. 8(a)-1A, area 1). This "bulb" has been cut open to expose interior layering (photo taken at noon on June 24, 2006). The entire mat cover in the creek channel was eroded during a rainstorm on June 18, 2006, and new growth starts at that surface (red arrow). From June 22 (turquoise arrow) to June 23 (yellow arrow), 2006 a series of rain showers moved across the area over a 24 hour period. Because individual rainfall events were not as severe, multiple pulses of surface runoff moved sand and clay through the creek channel, but caused little or no erosion of prior mat growth. The corresponding mat layer (between turquoise and yellow arrow) is darkened by sediment grains. The mat layer bracketed by the yellow and black arrows formed over a time period of approximately 24 hours following the end of overland flow on June 23. (F) The same area as shown in E, but 18 hours later. Mat growth has already obscured and softened the sharp rim seen in E. For easier location, the white arrows point to the same spots as marked with white arrows in E. (G) A closer view of the arrangement of *Leptothrix* sheaths in the Spurr resin matrix of the sample shown in D. Elongate and round features are iron hydroxide encrusted sheaths of *Leptothrix*. Their iron encrustation makes for the bright response in backscatter mode. (H) High magnification SEM image (backscatter mode) of same mat lamina as shown in G. Arrows point to *Gallionella* stalks.

In: *Atlas of microbial mat features preserved within the clastic rock record*, Schieber, J., Bose, P.K., Eriksson, P.G., Banerjee, S., Sarkar, S., Altermann, W., and Catuneau, O., (Eds.), Elsevier, p. 233-244. (2007)

References

Anderson C. R. and Pedersen K., 2003. In situ growth of Gallionella biofilms and partitioning of lanthanides and actinides between biological material and ferric oxyhydroxides. Geobiology 1, 169-178.

Baur M., Hayes J., Studley S., Walter M., 1985. Millimeter-scale variations of stable isotope abundances in carbonates from banded iron formations in the Hamersley Group of Western Australia. Econ. Geol. 80, 270-282.

Bazylinski D. A. and Frankel R. B., 2003. Biologically controlled mineralization in prokaryotes. Rev. Mineral. Geochem. 54, 217-247.

Christensen, P.R., R.N. Clark, H.H. Kieffer, M.C. Malin, J.C. Pearl, J.L. Bandfield, K.S. Edgett, V.E. Hamilton, T. Hoefen, M.D. Lane, R.V. Morris, R. Pearson, T. Roush, S.W. Ruff, and M.D. Smith, 2000, Detection of crystalline hematite mineralization on Mars by the Thermal Emission Spectrometer: Evidence for near-surface water, *J. Geophys. Res.*, *105*, 9623-9642, 2000.

Cloud P., 1973. Paleoecological significance of the banded iron-formation, Econ. Geol. 68, 1135-1143.

Cornell R. M. and Schwertmann U., 2003. The Iron Oxides: Structure, Properties, Reactions, Occurrences and Uses, 2nd, Completely revised and Extended Edition. Wiley-VCH Verlag, Weinheim, Germany, p.703.

Emerson D. and Weiss J. V., 2004. Bacterial iron oxidation in circumneutral freshwater habitats: findings from the field and the laboratory. Geomicrobiol. J. 21, 405-414.

Emerson D., Weiss J. V., Megonigal J. P., 1999. Iron-oxidizing bacteria are associated with ferric hydroxide precipitates (Fe-plaque) on the roots of the wetland plants. Appl. Environ. Microbiol. 65, 2758-2761.

Fortin D. and Langley S., 2005. Formation and occurrence of biogenic iron-rich minerals. Ear. Sci. Rev. 72, 1-19.

Fortin D., Tessier A., Leppard G. G., 1993. Characteristics of lacustrine iron oxyhydroxides. Geochim. Cosmochim. Acta 57, 4391-4404.

Gehling, JG, 1999, Microbial mats in terminal Proterozoic siliciclastics: Ediacaran death masks. Palaios, v. 14, p. 40–57.

Gerdes, G., and Krumbein, W.E., 1987, Biolaminated Deposits. Lecture Notes in Earth Sciences 9, Springer Verlag, New York, 183p.

Hallberg R. and Ferris F. G., 2004. Biomineralization by *Gallionella*. Geomicrobiol. J. 21, 325-330.

Hallbeck L. and Pedersen K., 1991. Autotrophic and mixotrophic growth of *Gallionella ferruginea*. J. Gen. Microbiol. 137, 2657-2661.

Holland H. D., 1973. The oceans: a possible source of iron in iron-formations. Econ. Geol. 68, 1169-1172.

Holm N. G., 1987. Possible biological origin of banded iron-formations. Econ. Geol. 68, 1169-1172/

Holm N.G., 1989. The 13C/12C ratios of siderite and organic matter of a modern metalliferous hydrothermal sediment and their implications for banded iron formations. Chem. Geol. 77, 41-45.

Isley A. E., 1995. Hydrothermal plumes and the delivery of iron to banded iron formation. J. Geol. 103, 169-185.

James R. and Ferris F. G., 2004. Evidence for microbial-mediated iron oxidation at a neutrophilic groundwater spring. Chem. Geol. 212, 301-311.
Kamber B. S., Bolhar R., Webb G. E., 2004. Geochemistry of late Archean stromatolites from Zimbabwe: evidence for microbial life in restricted epicontinental seas. Precambrian Res. 132, 379-399.
Kappler A. and Newman D. K., 2004. Formation of Fe(III)-minerals by Fe(II)-oxidizing photoautotrophic bacteria. Geochim. Cosmochim. Acta 68, 1217-1226.
Konhauser K. O., Hamade T., Raiswell R., Morris R. C., Ferris F.G., Southam G., Canfield D. E., 2002. Could bacteria have formed the Precambrian banded iron formations? Geology 30, 1079-1082.
LaBerge, G.L., 1973, Possible biological origin of Precambrian iron-formations. Economic Geology, v. 68, p. 1098–1109.
Little C. T. S., Glyn S.E.J., Mills R.A., 2004. Four-hundred and ninety-million-year record of bacteriogenic iron oxide precipitation at sea-floor hydrothermal vents. Geomicrobiol. J. 21, 415-429.
Lowenstam H. A., 1986. Mineralization processes in monerans and potoctists. In: Biomineralization in lower plants and animals. Vol. 30, Leadbeater B. S. C., Riding R. (eds) Oxford Uni. Press, New York, p. 1-17.
Morris R. C. and Horwitz R. C., 1983. The origin of the iron-formation-rich Hamersley Group of Western Australia – deposition on a platform. Precambrian Res. 21, 273-297.
Nealson K. H. and Myers C. R., 1990. Iron reduction by bacteria: a potential role in the genesis of banded iron formations. Am. J. Sci. 290-A, 35-45.
Pierson B. K., Parenteau M. N., Griffin B. M., 1999. Phototrophs in high-iron-concentration microbial mats: physiological ecology of phototrophs in an iron-depositing hot spring. Appl. Environ. Microbiol. 65, 5474-5483.
Rasmussen B. and Buick R., 1999. Redox state of the Archean atmosphere: evidence from detrital heavy metals in ca. 3250-2750 Ma sandstone from the Pilbara Craton, Australia. Geology 27, 115-118.
Reineck, H.-E., and Singh, I.B., 1980, Depositional and sedimentary environments, 2nd ed. Springer-Verlag, Berlin. 549pp.
Roden E. E., Sobolev D., Glazer B., Luther G. W., 2004. Potential for microscale bacterial Fe redox cycling at the aerobic-anaerobic interface. Geomicrob. J. 21, 379-391.
Schieber, J., 1989, Pyrite mineralization in microbial mats from the Mid-Proterozoic Newland Formation, Belt Supergroup, Montana, U.S.A.: Sedimentary Geology, v. 64, p. 79-90.
Schieber, J., 1999, Microbial Mats in Terrigenous Clastics: The Challenge of Identification in the Rock Record. Palaios, v. 14, p. 3-12.
Schieber, J., 2002, Sedimentary Pyrite: A window into the microbial past. Geology, v. 30, p. 531-534.
Simonson, BM, and Carney, KE, 1999, Roll-up structures: Evidence of in situ microbial mats in Late Archean deep shelf environments. Palaios, v. 14, p. 13–24.
Sobolev D. and Roden E. E., 2004. Characterization of a neutrophilic, chemolithoautotrophic Fe(II)-β-proteobacterium from fresh-water wetland sediments. Geomicrobiol. J. 21, 1-10.

Straub K.L, Benz M., Schrink B., 2001. Iron metabolism in anoxic environments at near neutral pH. FEMS Microbiol. Ecol. 34, 181-186.

Tipping E., Thompson D.W., Woof C., 1989. Iron oxides particulates formed by the oxygenation of natural and model lakewaters containing Fe(II). Arch. Hydrobiol. 115, 59-70.

In: *Atlas of microbial mat features preserved within the clastic rock record*, Schieber, J., Bose, P.K., Eriksson, P.G., Banerjee, S., Sarkar, S., Altermann, W., and Catuneau, O., (Eds.), Elsevier, p. 233-244. (2007)